Moroccan Journal of Chemistry
ISSN: 2351-812X
http://revues.imist.ma/?journal=morjchem&page=login
Al Moubaraki & al. / Mor. J. Chem. 8 N°1 (2020) 264-279

Investigation of the Corrosion Behavior of Mild Steel/H_2SO_4 Systems

Aisha H. Al-Moubaraki [(a)]*, Aisha A. Ganash [(b)], Salwa D. Al-Malwi [(b)]

[(a)] *Chemistry Department, Faculty of Science–Alfaisaliah Campus, University of Jeddah, Jeddah, Saudi Arabia*
[(b)] *Chemistry Department, Faculty of Science, King Abdulaziz University, Jeddah, Saudi Arabia*

** Corresponding author:*
ahmobaraki@uj.edu.sa
ahm13988@hotmail.com
Received 21 Jan 2020
Revised 13 Feb 2020
Accepted 29 Feb 2020

Abstract

The corrosion behavior and mechanism of mild steel/H_2SO_4 systems were examined using hydrogen gas evolution, HE, and weight loss, WL, as chemical measurements and electrochemical impedance spectroscopy, EIS, and potentiodynamic polarization, PDP, as electrochemical measurements at 30°C. From the chemical results, the corrosion rate of mild steel increased as well as increasing acid concentration, with a reaction constant of 0.70 and 0.60 for HE and WL, respectively. Different features including general and pitting corrosion can be shown on the mild steel surface after dipping in different concentrations of H_2SO_4, and the latter became more distinct at higher acid concentrations. EIS results showed that the R_p value decreases while the C_{dl} value increases along with increasing acid concentration. PDP results clearly revealed that the dissolution of mild steel undergoes anodic control. The chemical and electrochemical method suggested that the dissolution mechanism of mild steel is the same at different H_2SO_4 concentrations. Based on the results and observations, the mechanism of mild steel corrosion in H_2SO_4 can be explained based on the role of SO_4^{2-} anions, the main corrosive agent in aqueous H_2SO_4 solutions, which partake directly in anodic dissolution and cathodic reaction during corrosion.

Keywords: Corrosion, Sulfuric acid, Mild steel, pits, anodic control, SO_4^{2-} anions.

1. Introduction

Sulfuric acid, H_2SO_4 is a major ingredient in the chemical industry. Its common use in fertilizer manufacturing; although it plays a major role also in mineral processing, oil refining, wastewater processing, chemical synthesis, steel pickling, and other hydrometallurgical applications. Its vast end applications include as an ingredient in domestic acidic drain cleaners, as an electrolyte in lead-acid batteries, and in various cleaning agents [1]. On the other hand, the aggressive nature of this acid makes it attack the metallic materials used for storage tanks and pipes construction. Consequently, a wide range of metallic materials are used for constructing tanks and pipes depending on the concentration range of sulfuric acid [2]. Sulfuric acid has the unusual behavior that, while it acts as a non-oxidizing acid at low to rather high concentrations, it acts as a strong oxidizing acid when it becomes highly concentrated. Iron corrodes rapidly in low concentration of sulfuric acid, but passivates by forming a protective oxide layer in high concentrations [3]. Corrosion by sulfuric acid has received widespread interest by researchers, especially in the oil and gas industry, due to policies regarding the transformation of hydrogen sulfide (H_2S) and sulfur oxides (SO_x) that are produced during oil extraction and refining to sulfuric acid. such policies have been adopted to reduce the negative effects of aforementioned gases in the atmosphere as a result of fuel combustion, and thus to reduce global warming [2, 4] There are great economic incentives for the development of methods and materials that limit or reduce the corrosion of metallic structures. Such developments can only be achieved through a good understanding of the mechanisms and processes involved in this complex phenomenon. The current research aims to shed some light on the behavior and mechanism of mild steel corrosion in H_2SO_4 acid solutions (0.25-2.5 M) at 30°C. Different chemical and electrochemical measurements were performed for this purpose. In addition, surface structure of mild steel before and following dipping in different concentrations of H_2SO_4 acid solutions was certified with scanning electron microscopy (SEM).

2.Materials and Methods

2.1. Materials

The chemical structure of the mild steel specimens used for the corrosion tests was: 0.22% C, 0.70% Mn, 0.32% Si, 0.12% Cu, 0.09% Al, 0.04% Cr and the remainder is Fe. Mechanically cut specimens with dimensions length 4 cm and diameter 1 cm were used for chemical and electrochemical measurements, while specimens with dimensions 0.5 cm length and 1 cm diameter (disc) were used for SEM. For electrochemical experiments, the specimens were embedded in Teflon with a surface area of 0.972 cm^2 in interaction with the corrosive solutions. Prior to each experiment, the specimens were smooth using wet SiC papers in the range of 100-1200 then washed completely with deionized water, degreased with ethanol and then dried with a flow of air. Concentrated solutions of H_2SO_4 ranging from 0.25 to 2.50 M were prepared from analytical grade concentrated H_2SO_4 (98%) using deionized water.

2.2. Methods

2.2.1. Chemical (HE and WL) Measurements

Figure 1 presents the experimental set up used for chemical (hydrogen gas evolution, HE, and weight loss, WL) measurements. Fifty mL of each of the tested aggressive solutions was added into a cell of Mylius type connected to a calibrated burette filled with water through a polyethylene tube. Then a degreased, weighed mild steel specimen was cautiously thrown down into the tested solution and the cell was rapidly sealed to prevent leakage of hydrogen gas during the experiment. The time was recorded and the H_2 gas generated during the corrosion process was collected by descending movement of water at different time intervals of 90 minutes. The graphical plot of released H_2 gas per unit

area (mL cm^{-2}) against time (min) is a straight line. Thus, the hydrogen evolution rate (CR_{HE}) associated to corrosion rate was calculated from the slope of the straight line [5]:

$$CR_{HE} = \delta V / \delta t \quad (1)$$

At the ending of the experimental process, the mild steel specimen was disconnected from the examined solution, washed systematically with deionized water then ethanol, air stream dried, and then the weight checked again. The rate of weight loss (CR_{WL}) can be calculated using the variation in the weight of the specimen before and after immersion (ΔW) as well as the end time (t_∞), as follows [5]:

$$CR_{WL} = \frac{\Delta W}{A \times t_\infty} \quad (2)$$

where A is the surface area of the mild steel specimen. All experiments were duplicated and conducted in standing at 30°C.

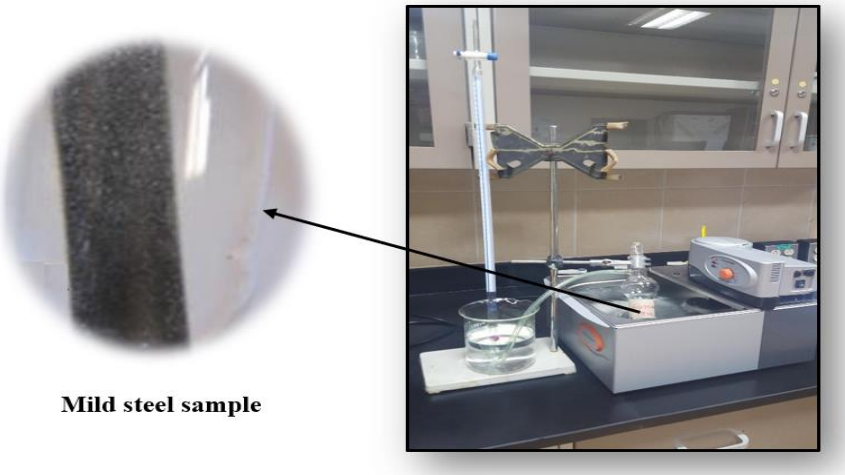

Figure 1. The system applied for chemical (HE and WL) measurements.

2.2.2. Electrochemical (EIS and PDP) Measurements

Electrochemical impedance spectroscopy, EIS, and potentiodynamic polarization, PDP, measurements were done with conventional electrochemical cell of three electrodes of 250 mL capacity. Mild steel, Ag/AgCl/KCl_{sat} electrode joined to a fine lugging capillary, and platinum wire served, respectively, as working, reference, and auxiliary electrodes. All electrochemical measurements were conducted through an ACM Gill AC instrument model 1649 in the following sequence: EIS→PDP in one test applying similar working electrode without additional surface treatment. All studied systems were stagnant, naturally aerated and maintained at 30°C. The EIS spectra were documented 10 min after the electrode was immersed to obtain steady state potential. A frequency range from 30 kHz to 0.5 Hz and an AC potential amplitude of 10 mV were applied. Cathodic and anodic polarization curves were recorded at a sweep rate of 1 mV s^{-1} and within the potential range from -700 to -200 mV. Electrochemical parameters derived from EIS measurements such as the solution resistance (R_s), the polarization resistance (R_p) and the double layer capacitance (C_{dl}) were anticipated by fitting the impedance data to the suitable equivalent circuit using the simulation tool of ZSimDemo 3.20 software. Using analysis software of ACM Gill 1649, the PDP parameters such as corrosion current density (i_{corr}), Tafel slopes (βa and βc), and corrosion potential (E_{corr}) can be estimated by applying the Tafel extrapolation approach. Each test was run twice, and the average value was taken.

2.2.3. Scanning Electron Microscopy (SEM) Examinations

Scanning electron microscopy was used to study the morphology of the mild steel surface before and after immersion in the different concentrations of H_2SO_4 .The surface samples were examined by a field emission scanning electron microscopy (FESEM), of model JSM-7500 F (JEOL – Japan).

3. Results and Discussion

3.1. Chemical (HE and WL) Measurements

The corrosion rate of the mild steel specimen was established by following the variation in the volume of evolved H_2 gas as a function of time when the specimen was reacting with various concentrations of H_2SO_4 in the range of (0.25-2.50) M at 30°C as shown in Figure 2. A linear increase of the volume of H_2 evolved (mL cm^{-2}) with time (min) can be observed in the Figure. Additionally, as the concentration of the acid increased, the slope of the linear relation also increased, indicating an increase in the corrosion rate. The good linearity in the relation indicates acceleration behavior of the mild steel dissolution because of the non-availability of an insoluble film on the metal surface through corrosion.

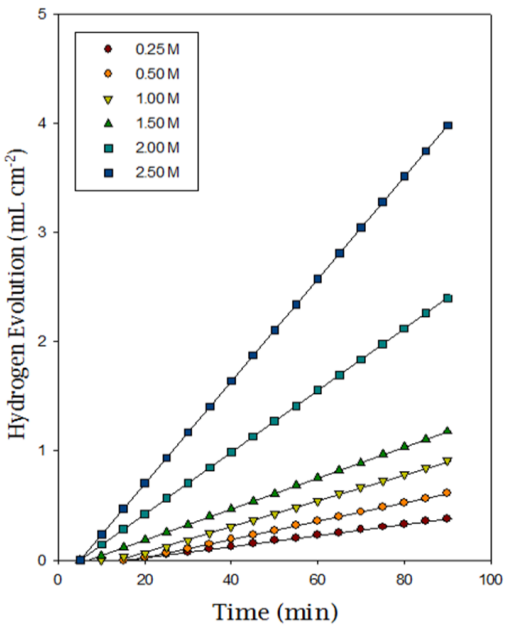

Figure 2. Hydrogen gas evolution dependance on time through mild steel corrosion in various concentrations of H_2SO_4 at 30°C.

Table 1 summarizes the corrosion rates (CR_{HE} and CR_{WL}) for the mild steel specimen in H_2SO_4 solutions of different concentrations obtained from HE and WL measurements, respectively. The results show that with increasing H_2SO_4 concentration, both CR_{HE} and CR_{WL} increase. This result is predictable because the passivating film in steel is probably Fe_2O_3. However, Fe_2O_3 is soluble below a pH of about 2. The pH is inversely proportional to the H^+ concentration, and thus a low or negative pH is associated with concentrated strong acids [3]. Figure 3 shows that this is true for the studied concentrations of sulfuric acid. As the hydrogen ion concentration increases, so pH decreases, and corrosion rate increases. Consequently, both the mild steel dissolution (anodic process) and the hydrogen gas evolution (cathodic process) increase.

Table 1. Corrosion rates obtaiend from both HE and WL for mild steel in various concentrations of H_2SO_4 at 30°C.

$C_{H_2SO_4}$ (M)	Corrosion Rates	
	$CR_{HE} \times 10^2$ mL cm^{-2} min^{-1}	$CR_{WL} \times 10^5$ g cm^{-2} min^{-1}
0.25	0.570	1.980
0.50	0. 870	2.450
1.00	1.310	3.488
1.50	1.760	4.519
2.00	2.610	6.690
2.50	2.790	7.890

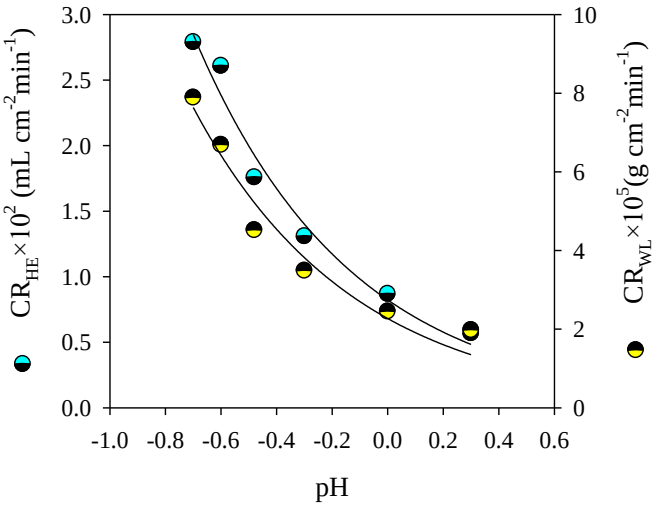

Figure 3. Corrosion rate dependence on pH for mild steel in various concentrations of H_2SO_4 at 30°C.

The corrosive nature of H_2SO_4 and its aqueous solutions were studied [2–4, 6–11]. It is well known that H_2SO_4 is a strong acid and dissociates in aqueous solutions as shown in the following equations [12]:

$$H_2SO_4 \rightarrow HSO_4^- + H^+ \quad Ka_1 \text{ is very high} \qquad \textbf{(3)}$$

$$HSO_4^- \leftrightarrow SO_4^{2-} + H^+ \quad Ka_2 = 1.2 \times 10^{-2} \qquad \textbf{(4)}$$

At low and medium acid concentrations, the dissociation is complete, and the predominant species is SO_4^{2-} which is a very corrosive agent for metals. At high concentrations, the dissociation is partial, and therefore the predominant species in solution is HSO_4^- which is not a very corrosive agent. According to that, the intensity of the anodic dissolution of steel in the studied acid concentrations (0.25-2.5 M) is dependent on the characteristic and concentration of the anion in the electrolyte, and the SO_4^{2-} anion is an active stimulant of this process and a major de-passivator. Mindyuk *et al.*, [11] reported that SO_4^{2-} anions are the main corrosion-active agent in aqueous H_2SO_4 solutions that directly participate in anodic and cathodic reactions during corrosion under stable conditions. Subsequently, the corrosion rate of H_2SO_4 acid solutions is ascertained majorly by SO_4^{2-}anions concentration. According to

Benamor *et al.*, [13], an increase in the SO_4^{2-} concentration accelerates the dissolution rate. The occurrence of accelerated corrosion of mild steel was attributed to the formation of complexes between SO_4^{2-} anions and iron.
The corrosion rate (CR_{HE} and CR_{WL}) as a function of the acid concentration can be used to show the rate dependence of H_2SO_4 acid concentration through the log-log plot which is in accordance with the following kinetic relations [14]:

$$CR = kC_{H_2SO_4}^{n} \quad (5)$$

$$\log CR = \log k + n \log C_{H_2SO_4} \quad (6)$$

Where k represents constant called the specific reaction rate, n is a constant for the reaction and $C_{H_2SO_4}$ is the molar concentration of H_2SO_4 solution. A plot of $log\ CR$ (for both HE and WL) against $log\ C_{H_2SO_4}$ gives straight lines with higher values of correlation coefficient, as demonstrated in Figure 4. The slopes of these lines are n and the intercepts are $logk$. The values of k can be regarded as the corrosion rate at unity concentration of H_2SO_4. The estimated k values from the above relation were about 1.278 $\times 10^{-2}$ mL cm^{-2} min^{-1} and 4.016 $\times 10^{-5}$ g cm^{-2} min^{-1}. These values are almost similar to the experimental result in Table 1 for mild steel corrosion in 1.0 M H_2SO_4 solution. The n values were 0.70 and 0.60 for, HE and WL, respectively. The larger the value of n, the greater the increase of the rate of corrosion reaction with the concentration of acid will be. In order to shed more light on the effect of H_2SO_4 acid concentrations on mild steel corrosion, morphological studies of mild steel surface were performed pre and post immersion in different concentrations of H_2SO_4 acid for 90 minutes at 30°C. The results are presented in Figure 5. Figure 5(a) illustrates the clean polished surface of mild steel before immersion in acid solutions. Parallel features with smooth scratch that are related to the mechanical polishing process can be observed. considering Figure 5(b-d), the mild steel surface was damaged and became very rough as a result of the aggressive attack of SO_4^{2-}anions. General and pitting corrosion was clearly observed and became more pronounced when the acid concentration increased. The pits had a small diameter and were partially regular at 0.25 M of H_2SO_4, while they had large diameter with irregular shapes and were full of corrosion products at 2.0 M of H_2SO_4. This finding agrees with the previous results of chemical measurements and confirms the increase in mild steel corrosion with increasing H_2SO_4 acid concentration.

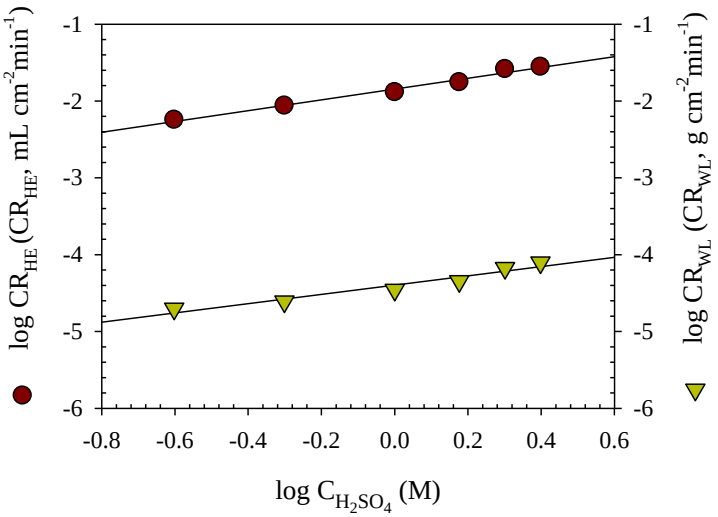

Figure 4. plot of *log* (CR_{HE} and CR_{WL}) *vs.* log $C_{H_2SO_4}$

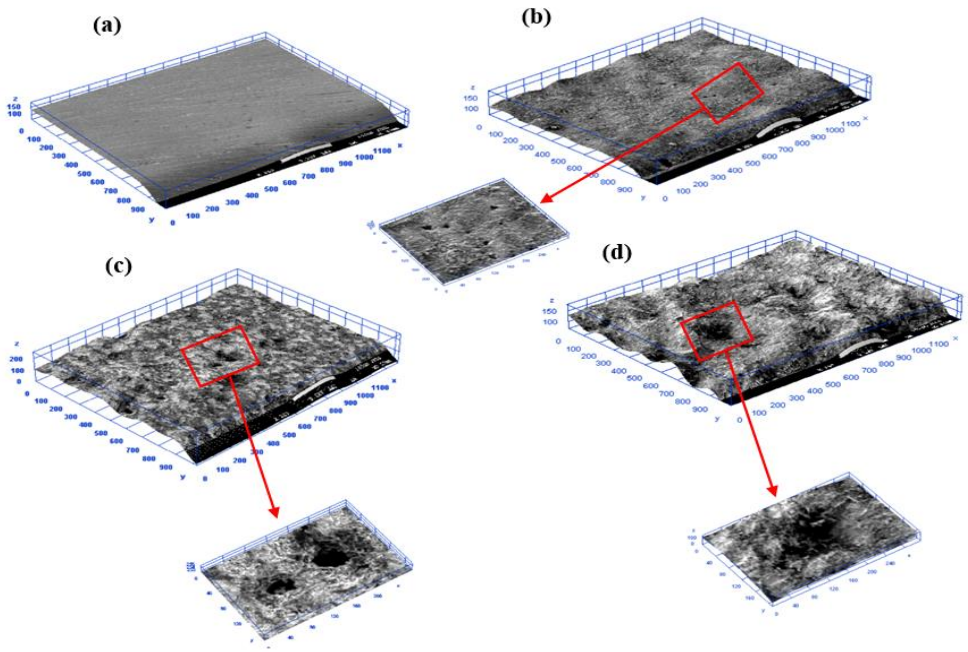

Figure 5. SEM images of unexposed and exposed mild steel for 90 minutes in various concentrations of H_2SO_4 at 30°C: (a) before immersion, and after immersion in (b) 0.25 M; (c) 1.0 M; and (d) 2.0 M.

3.2. Electrochemical Impedance Spectroscopy (EIS) Measurements

The impedance method gives data about the kinetics of the electrode processes and at the same time about the properties of the surface of the examined systems. Mechanistic information can be estimated from the structure of impedance [15]. Figure 6 represents the Nyquist plot for mild steel corrosion in different H_2SO_4 concentration at 30°C. It can be seen that there were no changes in the profile of the Nyquist plot at different studied concentrations, made up of a capacitive loop at high frequencies and a small inductive loop at low frequencies, implying that the corrosion mechanism is similar at the different studied acid concentrations. The high frequency capacitive loop is typically associated to the charge transfer (electron transfer) of the corrosion process and the subsequent double layer behavior [16]. Nevertheless, owing to the frequency dispersion resulting from the irregularity and non-homogeneity of electrode surface [17], the capacitive loop displays a depressed semicircle. In the meantime, the low frequency inductive loop normally occurs in the case of sever corrosive condition and is ascribed to the relaxation process produced by adsorption of species such as $(SO_4^{2-})_{ads}$ and $(H^+)_{ads}$ [17,18] on the mild steel specimen.

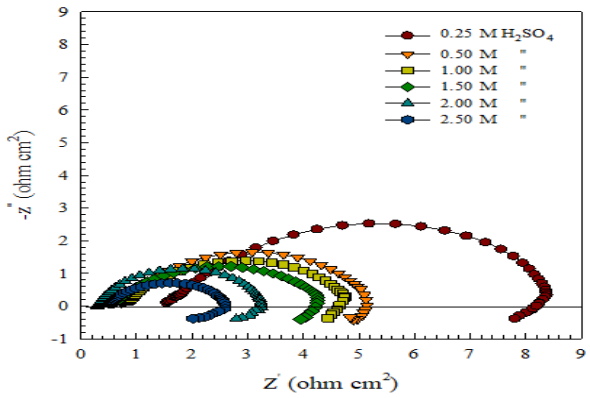

Figure 6. Nyquist plots of mild steel in various concentrations of H_2SO_4 at 30°C.

A major striking feature of impedance spectroscopy is the direct creation that often exists between the performance of a physical system and an perfect model circuit made up of discrete electrical components [19, 20]. Consequently, EIS data for mild steel corrosion in different H_2SO_4 concentrations were transferred to the simulation software program (ZSimDemo 3.20) with the sole aim of obtaining the fitting equivalent circuit (EC) and permitting the calculation of mathematical values which correspond to the physical and/or chemical properties of the investigated electrochemical system. Based on the features displayed by EIS data on Nyquist plot, the best EC model fit to all experimental EIS data is shown in Figure 7. In the adapted circuit, R_s, R_{ct}, and R_L represent the solution, charge transfer, and inductive resistances, individually, while L is the inductive elements. Additionally, the CPE is a constant phase element which is used to exchange a double layer capacitance for the non-homogeneity of the metal surface, which results to larger depression in the Nyquist semicircle chart and consequently perfect fitting. A number of studies have used an equivalent circuit to interpret data for metallic electrode in H_2SO_4 solutions [4,14-15,18].The inductance (L) and the inductive resistance (R_L) are correlated with intermediate processes at low frequencies. It must be noted that the Chi-squared (χ^2) is used to evaluate the fitting quality of the data where values are in the range $4.58 \times 10^{-4} \leq \chi^2 \leq 2.96 \times 10^{-3}$.This result reveals that the χ^2 values are low, which indicates that the fitted data are consistent with the experimental data.

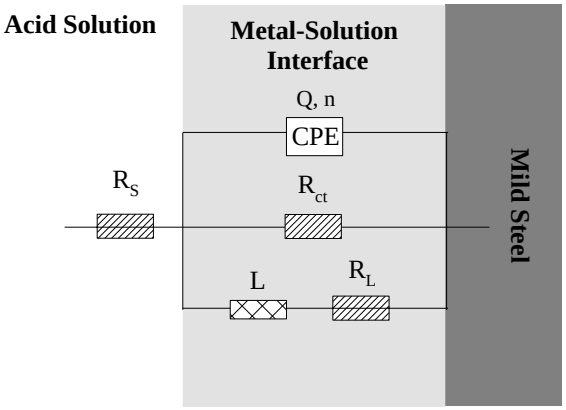

Figure 7. The equivalent circuit model employed to suit the experimental impedance data.

The polarization resistance R_p can be assessed with the below equation [22]:

$$R_p = \frac{R_{ct} \times R_L}{R_{ct} + R_L} \quad (7)$$

and the values of double layer capacitance (C_{dl}) can be obtained from CPE (Q) and (R_{ct}), with the below relation [23]:

$$C_{dl} = (Q.R_{ct}^{1-n})^{1/n} \quad (8)$$

The estimated values of R_s, R_p and C_{dl} are presented in Table 2. Interpretation of the results is as follows:

- Solution resistance (R_s) is often an important factor in the impedance of an electrochemical cell. It was found that R_s value depends on the ionic concentration of the solution. The highest R_s values were detected in low acid concentration (0.25M). A sudden decrease in the R_s value was observed with increased acid concentrations. This result is consistent with previous results obtained by Benamor *et al.*, [13] wherein the resistance values of the solution were decreased with the increase of SO_4^{2-} anion concentration.
- For an electrochemical estimation of the examined bare metal, two significant parameters were mainly considered: the double layer capacitance (C_{dl}) and the polarization resistance (R_p). Figures (8 a and b) show the effect of H_2SO_4 acid concentration on the values of C_{dl} and R_p. As was observed, the variations of the two parameters with acid

concentration had opposite trends. In another word, when the acid concentration increases, the polarization resistance tends to decrease, and the double layer capacitance increases. According to the electrochemical theory, the corrosion rate is inversely related to the polarization resistance and is directly related to the double layer capacitance. In accordance with this theory, From Figures (8 a and b), there is increased corrosion rate of mild steel with increasing acid concentration and this electrochemical behavior agrees well with the data obtained from chemical measurements.

Table 2. Corrosion parameters of mild steel obtained from EIS measurements in various concentrations of H_2SO_4 at 30ºC.

$C_{H_2SO_4}$ (M)	R_s (ohm cm^2)	R_p (ohm cm^2)	C_{dl} (µF cm^{-2})
0.25	1.614	6.891	244
0.50	0.741	5.306	457
1.00	0.765	4.503	643
1.50	0.589	3.904	875
2.00	0.298	2.905	1054
2.50	0.496	2.223	1265

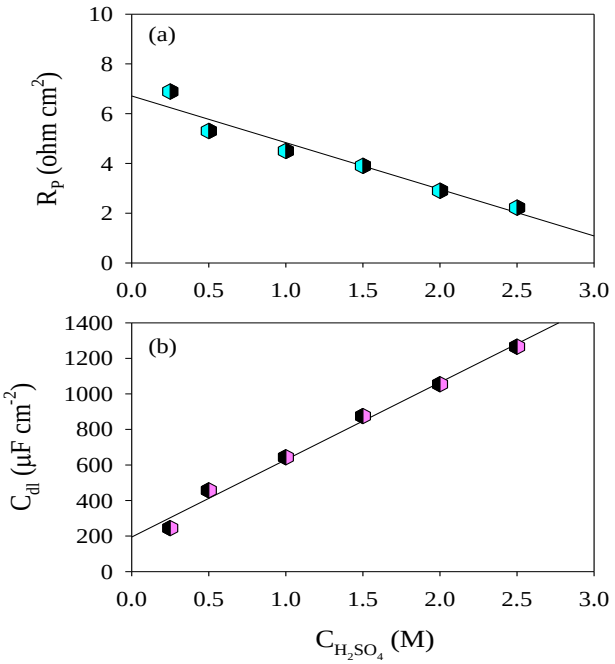

Figure 8. Variation of (a) R_p and (b) C_{dl} with $C_{H_2SO_4}$ at 30ºC.

3.3. Potentiodynamic Polarization (PDP) Measurements

Laboratory corrosion testing is often conducted using potentiodynamic polarization. This method provides important valuable information about mechanisms and rate of corrosion and sensitivity of certain materials to corrosion in specified environments. Figure 9 illustrates the effect of H_2SO_4 acid concentration on the anodic and cathodic polarization behavior of mild steel at 30ºC. The general shape of the potentiodynamic curves with the studied range of concentrations is relatively similar. However, with increasing acid concentration there was a shift in both anodic and

cathodic curves to higher current densities, while the corrosion potential (E_{corr}) experienced a shift to more positive values. Calculated values of the polarization parameters including corrosion potential (E_{corr}), anodic and cathodic Tafel slopes (βa and βc), and corrosion current density (i_{corr}), are presented in Table 3. The results interpretation is as follows:

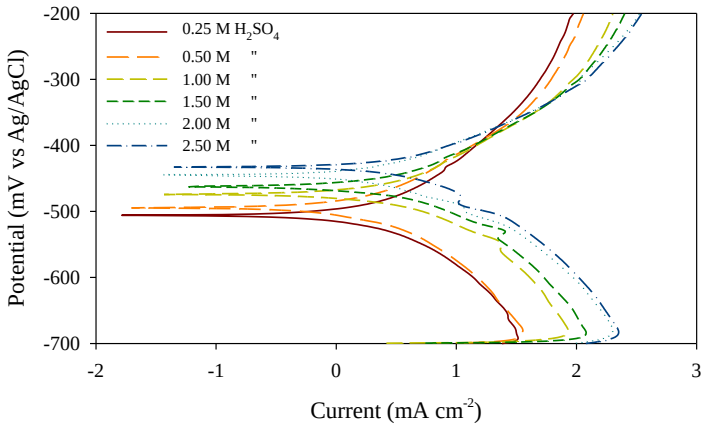

Figure 9. PDP curves of mild steel in various concentrations of H_2SO_4 at 30ºC.

Table 3. Corrosion parameters of mild steel obtained from PDP measurements in various concentrations of H_2SO_4 at 30ºC.

$C_{H_2SO_4}$ (M)	$-E_{corr}$ (V)	β_a (V.dec^{-1})	$-\beta_c$ (V.dec^{-1})	i_{corr} (mA cm^{-2})
0.25	0.507	0.087	0.092	3.65
0.50	0.495	0.084	0.093	4.70
1.00	0.471	0.082	0.090	6.23
1.50	0.462	0.085	0.090	7.67
2.00	0.445	0.085	0.092	9.69
2.50	0.433	0.083	0.090	11.80

- **Corrosion potential** (E_{corr}): values of E_{corr} experience shifts to more positive potentials along with increase of the H_2SO_4 acid concentration (anodic control).This can be explained using the mixed potential theory [24] by considering the contribution of both anodic and cathodic reactions in the corrosion process. Consequently, the positive shift in the values of E_{corr} reveals that the anodic process is considerably more influenced than the cathodic one [25]. As already noted, the anodic corrosion process in sulfuric acid solutions, which includes the movement of metal ions into solution, is obtained principally by the act of corrosion-active SO_4^{2-}anions, supported by the act of hydrogen ions which confirm the change of the electrode potential to more positive values; consequently leading to positive charging of the metal surface and rise in the adsorption rate of corrosion-active SO_4^{2-} anions on the cathodic (i.e., more negatively charged) areas of steel. Therefore, the discharge of hydrogen ions (decrease in cathodic control) is facilitated; which is an approval of the role of de-passivating influence of the anion [11]. The same behavior was reported by Sherif and Seikh [26] for dissolution of steel X70 in 1.0 M H_2SO_4 at different immersion periods. They attributed this behavior to the ability of the SO_4^{2-}anions to avoid the surface of steel to form coats of oxide and/or corrosion products that in turn permit the surface to undergo a continuous corrosion.

- **Corrosion current density** (i_{corr}): it is noticeable that the i_{corr} value increased and consequently the corrosion rate increased with increased H_2SO_4 acid concentration. Figure 10 depicts a linear relationship between E_{corr} and log i_{corr} for various concentrations of H_2SO_4 according to the equation [27]:

$$E_{corr} = a + b \log i_{corr} \quad (9)$$

Where a and b are constants characteristic of the reactivity of the metal, the reference electrode, and the temperature; and i_{corr} is a measure of the corrosion rate expressed in units of current density. It was observed that for a corroding specimen in various concentrations of H_2SO_4 , a change in the corrosion rate will produce a corresponding change in the E_{corr}. In the non-existence of significant coverage by adsorbed species, this change in E_{corr} is expected to be a degree of the change in the corrosion rate as the redox potential and concentration of the corrosion medium are varied.

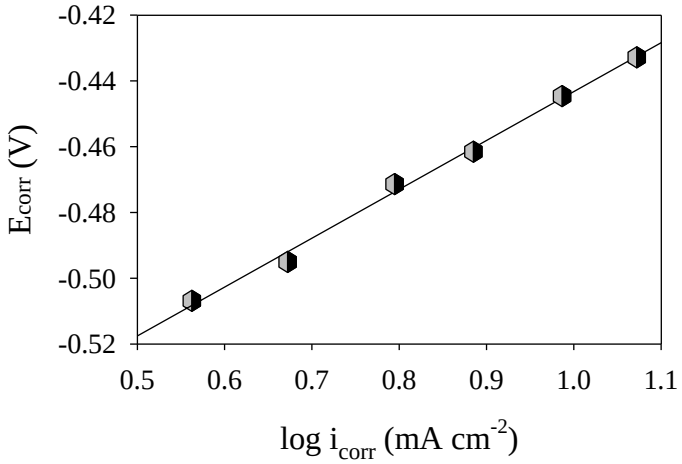

Figure 10. Variation of E_{corr} for mild steel with log i_{corr} at 30°C.

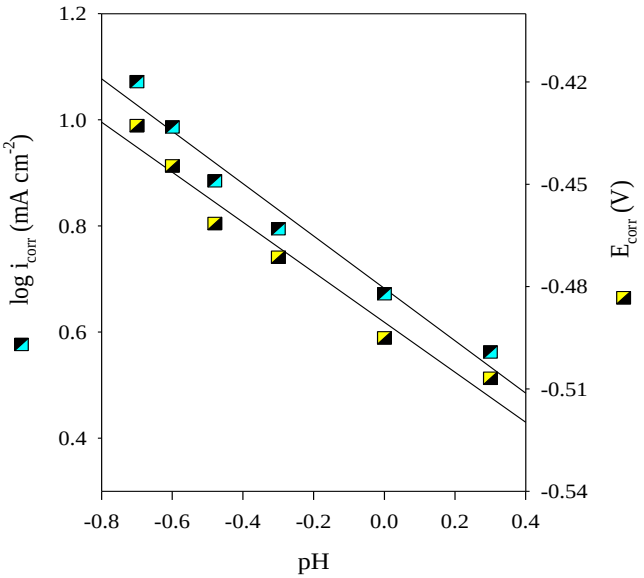

Figure 11. log i_{corr} and E_{corr} dependence on pH for mild steel in various concentrations of H_2SO_4 at 30°C.

The association of log i_{corr} and E_{corr} with pH are given in Figure 11. Linear relationships with high correlation coefficients were found for pH *vs*. E_{corr} and for pH *vs*. log i_{cor}. The differential value ($\delta E_{corr}/\delta pH$) determined based on Figure 11 was – 0.07 V, which is harmonious with the value in previous studies [10, 28]. This value has been mentioned extremely, while lower values (e.g. – 0.045 V [29]) have also been found. The value of (δ log i_{corr} /δ pH)

determined from Figure 11 was – 0.49 and is well consistent with the values stated by Bockris *et al.*, [28]. However, for this differential, various values, both positive and negative, have been reported [10]. These results confirm the increase in anodic dissolution rate of mild steel with decreasing pH (increasing acidity).

- **Tafel slopes** (β_a and β_c): As shown in Figure 9 and Table 3 the values of both β_a and β_c did not change significantly with increasing H_2SO_4 concentration. This implies that the mechanisms of anodic and cathodic reactions also does not change with increasing acid concentration [30]. This result is consistent with the previous suggestion in EIS measurements. Once the values of β_a and β_c are determined, the stern-Geary constant, B, can be calculated using the following equation [31]:

$$B = \frac{\beta_a \times |\beta_c|}{2.3(\beta_a + |\beta_c|)} \quad \textbf{(10)}$$

The polarization resistance ($R_{p\ (PDP)}$) can likewise be calculated from the Stern–Geary constant as follows:

$$R_{p\ (PDP)} = \frac{B}{i_{corr}} \quad \textbf{(11)}$$

By studying the R_p values obtained from EIS measurements and comparing them with those obtained from PDP measurements (Figure 12), a straight line can be viewed with a high correlation coefficient (r^2 = 0.98). Thus, we can conclude the R_p data from the two applied techniques were in good consistency.

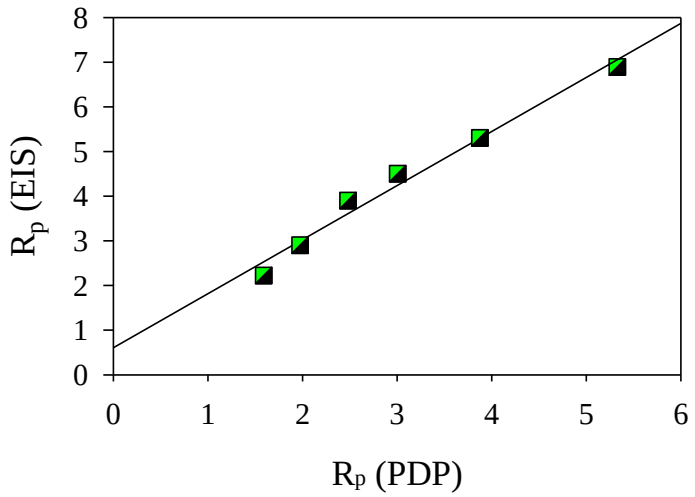

Figure 12. Correlation between R_p (EIS) and R_p (PDP).

3.4. Mechanism of Mild Steel Corrosion in H_2SO_4 Solutions

The behavior of mild steel corrosion in H_2SO_4 solution has established significant interest in the literature [2, 3, 11, 23,32–34]. The role of the SO_4^{2-}anions and other components in mild steel corrosion in H_2SO_4 solution must be considered. Accordingly, the corrosivity of H_2SO_4 solutions are determined by two main factors. The first is the concentration of SO_4^{2-} anions which determines the main corrosion phenomena progress, i.e., ions and electrons move from the metal to the solution. The second is the intensity of dissolution rate of the corrosion products, i.e., salt films formed on the steel surface, which count on the acid concentration. The minor corrosion processes, i.e., the removal of the surface salt films after damaged by water molecules, comprise the hydration, diffusion, and migration of their compounds into the solution. Dehydration of SO_4^{2-}anions is accompanied with electrostatic adsorption on the mild steel surface. As a result of electrostatic interaction, and due to the attraction of double bonds to protons, a complex double layer of metal surface-anions-hydrogen ions may be developed. Both the electrostatic adsorption of SO_4^{2-}

anions on the metal surface with unfilled d-levels and the creation of a complex double layer reduce the work function of the metal thus facilitating hydrogen ions discharge, i.e., reduce the excess voltage needed for hydrogen evolution. As a result of this loss of electrons, the metal turn into positively charged, anion adsorption is enhanced, and so is the process of metal ions flow into solution. The above discussion of the role of SO_4^{2-}anions on corrosion of mild steel in H_2SO_4 solutions can be explained according to electrons exchange by metal oxidation (anodic reaction) and hydrogen reduction (cathodic reaction) with the following reactions, separately [35]:

Anodic reaction $$Fe \rightarrow Fe^{2+} + 2e^- \quad \textbf{(12)}$$

Cathodic reaction $$2H^+ + 2e^- \rightarrow H_2 \uparrow \quad \textbf{(13)}$$

In the presence of SO_4^{2-}anions in aqueous solutions, several mechanisms on the anodic dissolution of iron have been assumed.

(i) Primary (main) corrosion Mechanism [34]:

$$(H_2O)_{ads} + SO_4^{2-} \leftrightarrow H_2O + (SO_4^{2-})_{ads} \quad \textbf{(14a)}$$

$$Fe + SO_4^{2-} \leftrightarrow (FeSO_4^{2-})_{ads} \quad \textbf{(14b)}$$

$$(FeSO_4^{2-})_{ads} \leftrightarrow (FeSO_4)_{ads} + 2e^- \quad \textbf{(14c)}$$

$$(FeSO_4)_{ads} \leftrightarrow Fe^{2+} + SO_4^{2-} \quad \textbf{(14d)}$$

In the presence of SO_4^{2-} anions, reaction (**14b**) progresses on the metal surface rapidly. Therefore, the dissolution of iron (anodic reaction) was main controlled by both electro-dissolution of iron and diffusion of soluble $(FeSO_4)_{ads}$ to the bulk solution. The anodic dissolution of iron in aqueous solutions including SO_4^{2-}anions may also involve the formation of adsorbed intermediate $[FeSO_4OH]_{ads}^{2-}$. Therefore, the below reactions contribute to iron dissolution.

(ii) Secondary (minor) corrosion mechanism [30, 36]:

$$Fe + SO_4^{2-} + H_2O \leftrightarrow [FeSO_4OH]_{ads}^{2-} + H^+ + e^- \quad \textbf{(15a)}$$

$$[FeSO_4OH]_{ads}^{2-} \leftrightarrow [FeSO_4OH]_{ads}^{-} + e^- \quad \textbf{(15b)}$$

$$[FeSO_4OH]_{ads}^{-} + H^+ \leftrightarrow Fe^{2+} + SO_4^{2-} + H_2O \quad \textbf{(15c)}$$

The cathodic hydrogen gas evolution (HE) reaction might be described as follows [37]:

- principal discharge stage (Volmer reaction)

$$Fe + H_3O^+ + e^- \leftrightarrow (FeH)_{ads} + H_2O \quad \textbf{(16)}$$

- an electrochemical-desorption stage (Heyrovsky reaction)

$$(FeH)_{ads} + H_3O^+ + e^- \rightarrow Fe + H_2 \uparrow + H_2O \quad \textbf{(17)}$$

- a recombination stage (Tafel reaction)

$$(FeH)_{ads} + (FeH)_{ads} \rightarrow 2Fe + H_2 \uparrow \quad \textbf{(18)}$$

In acidic media, the hydrogen atoms that are absorbed $(FeH)_{ads}$ will recombine to form hydrogen molecules, which rise as bubbles on the metal surface. This process is the second stage of the cathodic reaction (HE). This stage can happen via an atom-atom combination as suggested by the chemical recombination mechanism (Tafel-Volmer) or an ion-atom reaction as suggested by the electrochemical recombination mechanism (Volmer-Heyrovsky) [37].

4. Conclusion

- Corrosion rates (CR_{HE} and CR_{WL}) of mild steel increase with increasing H_2SO_4 concentration.
- Morphology studies for mild steel after dipping in different concentrations of H_2SO_4 solutions displayed general and pitting corrosion and the latter became more distinct at higher levels of H_2SO_4 concentration.

- EIS measurements showed that R_p values decrease while C_{dl} values increase with increasing H_2SO_4 concentration.
- PDP results revealed that the mild steel corrosion is under anodic control.
- Chemical and electrochemical measurements suggested that the corrosion mechanism of mild steel is the same at the different studied H_2SO_4 concentrations.
- Based on the findings and explanations, the mechanism of mild steel corrosion in H_2SO_4 can be described according to the role of SO_4^{2-} anions, the main corrosion-active agent in aqueous H_2SO_4 solutions, which play a precise part in anodic dissolution and cathodic reaction during corrosion.

References

[1] H. Müller, Sulfuric Acid and Sulfur Trioxide., in: *Ullmann's Encycl. Ind. Chem.*, Wiley-VCH Verlag GmbH & Co. KGaA, Weinheim, Germany, 2000: pp. 1–71. doi:10.1002/14356007.a25_569.

[2] Z. Panossian, N.L. de Almeida, R.M.F. de Sousa, G. de S. Pimenta, L.B.S. Marques, Corrosion of carbon steel pipes and tanks by concentrated sulfuric acid: A review, *Corros. Sci.* 58 (2012) 1–11. doi:10.1016/j.corsci.2012.01.025.

[3] G.W.P. Rengstorff, K. Miyoshi, D.H. Buckley, Friction and Wear of Iron in Sulfuric Acid, *Natl. Aeronaut. Sp. Adm.* (1984) 1–19.

[4] M. Ferhat, A. Benchettara, S.E. Amara, D. Najjar, Corrosion behaviour of Fe-C alloys in a sulfuric medium, *J. Mater. Environ. Sci.* 5 (2014) 1059–1068.

[5] E.A. Noor, A. Al-Moubaraki, A.H. Al-Zhrani, M.H. Hubani, Testing and Comparing The Tnhibitory Action of Red Onion Seeds and Peels Extracts on The Corrosion of Steel in Phosphoric Acid, *Int. J. Electrochem. Sci.* 11 (2016) 6523 – 6539. doi:10.20964/2016.08.47.

[6] J.G. Hines, R.C. Williamson, Anodic behaviour of mild steel in strong sulphuric acid-I. Steady-state conditions, *Corros. Sci.* 4 (1964) 201–210. doi:10.1016/0010-938X(64)90019-8.

[7] S. Mischer, E. Rosset, G.W. Stachowiak, D. Landolt, Effect of sulphuric acid concentration on the rate of tribocorrosion of iron, *Wear.* 167 (1993) 101–108. doi:10.1016/0043-1648(93)90314-C.

[8] M.A. Azam, M.F. Ibrahim, M. Zaimi, Corrosion Analysis of Carbon Steel Pipeline: Effect of Different Sulfuric Acid Concentrations, *Appl. Mech. Mater.* 699 (2014) 215–220. doi:10.4028/www.scientific.net/amm.699.215.

[9] Z.A. Foroulis, H.H. Uhlig, Effect of Velocity and Oxygen on Corrosion of Iron in Sulfuric Acid, *J. Electrochem. Soc.* 111 (2007) 13–17. doi:10.1149/1.2426050.

[10] M. Vuković, Influence of pH on the dissolution kinetics of iron in sulphuric acid solutions, *Hydrometallurgy.* 43 (1996) 79–93. doi:10.1016/0304-386x(96)00019-9.

[11] A.K. Mindyuk, E.I. Svist, O.P. Savitskaya, L.N. Petrov, Z.M. Outman, Corrosion activity of aqueous sulfuric acid solutions, *Fiz. Makhanika Mater.* 3 (1967) 157–164.

[12] H. Sippola, P. Taskinen, Thermodynamic properties of aqueous sulfuric acid, *J. Chem. Eng. Data.* 59 (2014) 2389–2407. doi:10.1021/je4011147.

[13] Y. Benamor, L. Bousselmi, H. Takenouti, E. Triki, Influence of sulphate ions on corrosion mechanism of carbon steel in calcareous media, *Corros. Eng. Sci. Technol.* 40 (2005) 129–136. doi:10.1179/174327805X29886.

[14] P.B. Mathur, T. Vasudevan, Reaction Rate Studies for the Corrosion of Metals in Acids, I. Iron in Mineral Acids, *Corrosion-NACE.* 38 (1982) 171–178. doi:10.5006/1.3580837.

[15] A.K. Singh, S.K. Shukla, M.A. Quraishi, Corrosion behaviour of mild steel in sulphuric acid solution in presence of ceftazidime, *Int. J. Electrochem. Sci.* 6 (2011) 5802–5814.

[16] X. Zheng, M. Gong, Q. Li, L. Guo, Corrosion inhibition of mild steel in sulfuric acid solution by loquat (Eriobotrya japonica Lindl.) leaves extract, *Sci. Rep.* 8 (2018) 1–15. doi:10.1038/s41598-018-27257-9.

[17] D. Daoud, T. Douadi, H. Hamani, S. Chafaa, M. Al-Noaimi, Corrosion inhibition of mild steel by two new S-heterocyclic compounds in 1 M HCl: experimental and computational study, *Corros. Sci.* 94 (2015) 21–37. https://www.sciencedirect.com/science/article/pii/S0010938X15000360 (accessed August 6, 2019).

[18] A.A. Al-Amiery, F.A. Binti Kassim, A.A.H. Kadhum, A.B. Mohamad, Synthesis and characterization of a novel eco-friendly corrosion inhibition for mild steel in 1 M hydrochloric acid, *Sci. Rep.* 6 (2016) 1–13. doi:10.1038/srep19890.

[19] X. Zheng, S. Zhang, W. Li, M. Gong, L. Yin, Experimental and theoretical studies of two imidazolium-based ionic liquids as inhibitors for mild steel in sulfuric acid solution, *Corros. Sci.* 95 (2015) 168–179. https://www.sciencedirect.com/science/article/pii/S0010938X15001390 (accessed August 6, 2019).

[20] W. Lai, Impedance Spectroscopy as a Tool for the Electrochemical Study of Mixed Conducting Ceria, Diss. (Ph.D.), California, *Inst. Technol.* (2007).

[21] E.A. Noor, A.H. Al-Moubaraki, A.A. Al-Ghamdi, Continuous Studies on Using Camel's Urine as Nontoxic Corrosion Inhibitor–Corrosion Inhibition of Al–Cu Alloy in Alkaline Solutions, *Arab. J. Sci. Eng.* 44 (2019) 237–250. doi:10.1007/s13369-018-3489-3.

[22] S.S. Abd El Rehim, H.H. Hassan, M.A. Amin, Corrosion inhibition study of pure Al and some of its alloys in 1.0 M HCl solution by impedance technique, *Corros. Sci.* 46 (2004) 5–25. https://www.sciencedirect.com/science/article/pii/S0010938X03001331 (accessed August 11, 2019).

[23] L. Bammou, M. Belkhaouda, R. Salghi, O. Benali, A. Zarrouk, H. Zarrok, B. Hammouti, Corrosion inhibition of steel in sulfuric acidic solution by the Chenopodium Ambrosioides extracts, *J. Assoc. Arab Univ. Basic Appl. Sci.* 16 (2014) 83–90. doi:10.1016/j.jaubas.2013.11.001.

[24] J.R. Scully, Corrosion, Electrochemical Principles of, in: *Encycl. Mater. Sci. Technol.*, 2004: pp. 1681–1686. doi:10.1016/b0-08-043152-6/00296-5.

[25] A. El-Sayed, Phenothiazine as inhibitor of the corrosion of cadmium in acidic solutions, *J. Appl. Electrochem.* 27 (1997) 193–200. doi:10.1023/A:1018456008267.

[26] E.M. Sherif, A.H. Seikh, Anodic dissolution in sulfuric acid pickling solutions of the API pipeline X70 grade steel, *Int. J. Electrochem. Sci.* 10 (2015) 209–222.

[27] W.E. Reid, Dissolution of iron in sulfuric acid solutions, *Corrosion-NACE.* 27 (1971) 407–417.

[28] J.O. Bockris, D. Drazic, A.R. Despic, The Electrode kinetics of the deposition and dissolution of iron, *Electrochim. Acta.* 4 (1961) 325–361. doi:10.1016/0013-4686(62)87007-8.

[29] K. Chandrasekara Pillai, R. Narayan, Anodic dissolution of mild steel in HCl solutions containing thio-ureas, *Corros. Sci.* 23 (1983) 151–166. doi:10.1016/0010-938X(83)90113-0.

[30] E.A. Noor, A.H. Al-Moubaraki, Corrosion behavior of mild steel in hydrochloric acid solutions, *Int. J. Electrochem. Sci.* 3 (2008) 806–818.

[31] M. Stern, A.L. Geary, Electrochemical Polarization I. A Theoretical Analysis of the Shape of Polarization Curves, *J. Electrochem. Soc.* 104 (1957) 56–63. doi:10.1149/1.2428653.

[32] E.C. Gan, M.E. Orazem, A Mathematical Model for the Corrosion of Iron in Sulfuric Acid, *J. Electrochem. Soc.* 134 (1987) 1357–1366. doi:10.1149/1.2100673.

[33] B.T. Ellison, Corrosion of Steel in Concentrated Sulfuric Acid, *J. Electrochem. Soc.* 125 (2006) 524. doi:10.1149/1.2131491.

[34] Y. Zhou, S. Zhang, X. Luo, B. Xiang, L. Guo, S. Kaya, Corrosion control of mild steel in 0.1 M H_2SO_4 solution by benzimidazole and its derivatives: An experimental and theoretical study, *RSC Adv.* 7 (2017) 23961–23969. doi:10.1039/C7RA02192E.

[35] S. Lyon, Overview of corrosion engineering, science and technology, in: *Nucl. Corros. Sci. Eng.*, Woodhead Publishing, 2012: pp. 3–30. doi:10.1533/9780857095343.1.3.

[36] D.R. MacFarlane, S.I. Smedley, The dissolution Mechanism of iron in Chloride solutions, *J. Electrochem. Soc.* 133 (1986) 2240–2244.

[37] N.F. Atta, A.M. Fekry, H.M. Hassaneen, Corrosion inhibition, hydrogen evolution and antibacterial properties of newly synthesized organic inhibitors on 316L stainless steel alloy in acid medium, *Int. J. Hydrogen Energy*. 36 (2011) 6462–6471. doi:10.1016/j.ijhydene.2011.02.134.